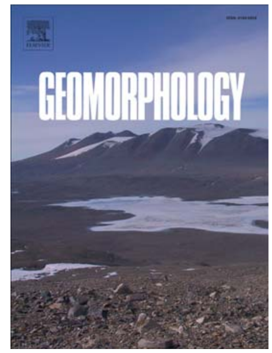

Permafrost and snow monitoring at Rothera Point (Adelaide Island, Maritime Antarctica): Implications for rock weathering in cryotic conditions

Mauro Guglielmin, M. Roger Worland, Fabio Baio, Peter Convey

PII: S0169-555X(14)00189-5
DOI: doi: 10.1016/j.geomorph.2014.03.051
Reference: GEOMOR 4737

To appear in: *Geomorphology*

Received date: 29 July 2013
Revised date: 25 March 2014
Accepted date: 27 March 2014

Permafrost and snow monitoring at Rothera Point (Adelaide Island, Maritime Antarctica): implications for rock weathering in cryotic conditions.

Mauro Guglielmin[1], M. Roger Worland [2], Fabio Baio[1]; Peter Convey [2]*

[1] *Dept. Theoretical and Applied Sciences, Insubria University, 21100 Varese, Italy*
**corresponding author: mauro.guglielmin@uninsubria.it*
[2] *British Antarctic Survey, NERC, High Cross, Madingley Road, Cambridge CB3 0ET, United Kingdom*

Abstract

In February 2009 a new permafrost borehole was installed close to the British Antarctic Survey Station at Rothera Point, Adelaide Island (67.57195°S 68.12068°W). The borehole is situated at 31 m asl on a granodiorite knob with scattered lichen cover. The spatial variability of snow cover and of ground surface temperature (GST) is characterised through the monitoring of snow depth on 5 stakes positioned around the borehole and with thermistors placed at three different rock surfaces (A, B and C) . The borehole temperature is measured by 18 thermistors placed at different depths between 0.3 and 30 m. Snow persistence is very variable both spatially and temporally with snow free days per year ranging from 13 and more than 300, and maximum snow depth varying between 0.03 and 1.42 m. This variability is the main cause of high variability in GST, that ranged between -3.7 and -1.5°C. The net effect of the snow cover is a cooling of the surface. Mean annual GST, mean summer GST, and the degree days of thawing and the n-factor of thawing were always much lower at sensor A where snow persistence and depth were greater than in the other sensor locations. At sensor A the potential freeze-thaw events were negligible (0-3) and the thermal stress was at least 40% less than in the other sensor locations. The zero curtain effect at the rock surface occurred only at surface A, favouring chemical weathering over mechanical action. The active layer thickness (ALT) ranged between 0.76 and 1.40 m. ALT was directly proportional to the mean air temperature in summer, and inversely proportional to the maximum snow depth in autumn. ALT temporal variability was greater than reported at other sites at similar latitude in the Northern Hemisphere, or with the similar mean annual air temperature in Maritime Antarctica, because vegetation and a soil organic horizon are absent at the study site. Zero annual amplitude in temperature was observed at about 16 m depth, where the mean annual temperature is -3°C. Permafrost thickness was calculated to range between 112 and 157 m, depending on the heat flow values adopted. The presence of sub-sea permafrost cannot be excluded considering the depth of the shelf around Rothera Point and its glacial history.

Introduction

Antarctica is considered a key area for understanding global climate and is the continent least disturbed by human activities. Although climate change in Antarctica over the last century is less well known than in other areas of the world, several studies have identified enhanced warming in the Antarctic Peninsula region, with an increase of 3.4°C in the mean annual air temperature and a greater value - 6.0°C - in winter temperature over the past 50 yr, making the region one of the world's climate warming “hotspots” (Vaughan et al., 2003; Turner et al., 2005, 2009, 2013).

Coupled with this rapid rate of regional atmospheric warming, dramatic retreat of most Antarctic Peninsula glaciers and collapse of ice shelves have occurred (e.g. Rott et al., 1996; Cook et al., 2005; Chapman and Walsh, 2007; Turner et al., 2007; 2013).

Permafrost response to these levels of warming remains poorly known and, in general, studies have been limited to the active-layer thermal regime or thickness change (e.g. Guglielmin, 2006; Ramos and Vieira, 2003; Ramos et al., 2007; Adlam et al., 2010; Guglielmin et al., 2012a). In both Antarctica and the Arctic, these are related to air temperature (Cannone et al., 2006; Guglielmin, 2004, 2006; Romanovsky et al., 2007; Adlam et al., 2010; Throop et al., 2012) and snow cover (Zhang and Stamnes, 1998; Guglielmin, 2004, 2006; Guglielmin and Cannone, 2012; Morse et al., 2012; Johansson et al., 2013), although incoming radiation can be important, especially on bare ground surfaces (Adlam et al., 2010; Guglielmin and Cannone, 2012). Differences in snow cover can drive large ground surface temperature variability (eg. Goodrich, 1982; Zhang, 2005; Ling and Zhang, 2006; Cook et al., 2008; Streletsky et al., 2008) and also variation in weathering rates (e.g. Ballantyne et al., 1985; Benedict, 1993; Hall, 1993; Matsuoka and Murton, 2008) and in ecosystem development (Chapin et al., 1995; Sturm et al., 2001, 2005; Guglielmin et al., 2012a; Paudel and Andersen, 2013). However studies documentating in detail the variability in snow cover, ground surface temperature (GST) and their relationships are rare in Antarctica (Guglielmin, 2006; Guglielmin and Cannone, 2012; Guglielmin et al., 2011; De Pablo et al., 2013).

The Antarctic scientific community has recognised the importance of permafrost and active layer thickness as potential indicators of climate change, and supported the creation of the Antarctic permafrost and soils (ANTPAS) group under the SCAR Geosciences Standing Scientific Group. Recently Vieira et al. (2010) summarised the progress of permafrost research in Antarctica carried out under the ANTPAS umbrella. Within the same framework, international cooperation between United Kingdom and Italy led to the installation of a borehole for permafrost monitoring at Rothera Research Station on Adelaide Island, west of the Antarctic Peninsula. Based on data obtained from the Rothera borehole site, the main aims of this paper are: (1) to analyse the spatial variability of snow cover and ground surface temperature, and their relationships, in order to understand their potential geomorphic implications, 2) to describe the permafrost temperatures and active layer thermal regime, and identify the relationships between the main climatic forcing factors and active layer thickness changes.

Study Area

The study site is located at Rothera Point, Adelaide Island (67°34′S; 68°07′W) in Marguerite Bay, southern Maritime Antarctic (Fig.1a). The area experiences a cold dry maritime climate (Ochyra et al., 2008), with a mean annual air temperature of -4.2 °C and mean annual precipitation of about 500 mm (Turner et al., 2002). Rothera Point is a rocky promontory with an ice-free area of c. 1000×250 m. The bedrock is quite homogeneous, composed of diorite and granodiorite of mid-Cretaceous to early Tertiary age (Dewar, 1970). The deglaciation age of the Rothera Point area is still not well known, although Emslie (2001) estimated that deglaciation occurred about 6000 yr BP. Permafrost is probably continuous, although detailed spatial and thermal data are lacking. Rock surfaces are generally covered by a diversity of epilithic lichens (dominated by *Usnea sphacelata* and *Umbilicaria decussata*) that can strongly influence weathering processes (Convey and Smith, 1997; Guglielmin et al., 2012b). The borehole site is located on a bedrock knob close to the "Memorial" on one of the highest summits of the Point (Fig. 1b).

Methods

Drilling was undertaken using a compressed and refrigerated air-driven drill and a ‘rockhammer’ drill bit. Drill cuttings were sampled at 1 m intervals for determination of mineralogical and thermal properties. The borehole is 101mm in diameter and, in order to prevent any water infiltration, an

HDPE tube sealed at the bottom was installed as a casing. Within the borehole 23 CS109 (Campbell Scientific) thermistors with an accuracy of 0.1°C were installed at depths of 0.3, 0.6, 0.8, 1,1.3, 1.6, 2.6, 5, 7, 9, 10, 11, 12, 13, 14, 15, 16, 18, 21, 24, 26, 28, 30 m and wired into a CR1000 datalogger (Campbell Scientific). In addition three thermistors were installed at 2 cm depth in three different adjacent locations to quantify spatial variability in the ground surface temperature (GST). One thermistor was installed very close to the borehole (Fig. 2a) on a subhorizontal rock surface (A) while the other two were installed further away, respectively on a subhorizontal (B) and a subvertical rock surface (C, Fig. 2b). Temperatures at the surface and down to 1.3 m depth in the borehole were recorded hourly while, at deeper depths, daily minimum, maximum and mean values were recorded. Snow depth was measured weekly visually on 5 stakes. The stakes are marked every 0.1 m, giving a measurement accuracy of ± 0.02 m. The stakes were also photographed on each measurement occasion.

The thermal diffusivity and specific heat of the granodiorite sampled in the borehole were measured in the laboratories of NETZSCH-Gerätebau GmbH (Selb, Germany) using a NETZSCH model 457 MicroFlashTM laser flash diffusivity apparatus equipped with a high-temperature furnace capable of operation from -125°C to 500°C. The sample chamber is isolated from the heating element by a protective tube allowing samples to be tested under vacuum or in an oxidizing, reducing or inert atmosphere. The thermal diffusivity measurements were conducted in a dynamic helium atmosphere at a flow rate of c. 100 ml/min between -3°C and 0°C. A standard sample holder for samples with a diameter of 0.0126 m was used. The temperature rise on the back face of the sample was measured using an InSb/MCT detector. The samples were coated with graphite on the front and rear surfaces in order to increase absorption of flash light on the front surface of the samples and to increase emissivity of the rear surface. The data presented are the mean of 5 individual tests.

The standard deviation of five shots at each temperature was less than 2%. The specific heat capacity was measured using the ratio method of ASTM-E 1461 (ASTM, 2007) with an accuracy of better than 5%. The system was calibrated with a standard material (Pyroceram, 0.0127m diameter, 0.002 m thick). The density of the rock at room temperature was determined using the buoyancy flotation method with an accuracy better than 5%. Thermal conductivity was calculated following Carlsaw and Jaeger (1959):

$$l = r * c_p * k \quad (1)$$

where l is the thermal conductivity (W m^{-1} K^{-1}), r is the bulk density (g cm^{-3}), c_p is the specific heat capacity (J g^{-1} K^{-1}) and k is the thermal diffusivity (m^2 s^{-1}).

Thermal diffusivity was also calculated at different depth intervals using the borehole measurements following Carlsaw and Jaeger (1959), applying the amplitude attenuation with depth (Equation 2) and the phase lag with depth (Equation 3):

$$ka = \pi/P\ [(z_2-z_1)/Ln\ (A_1/A_2)]^2 \quad (2)$$

$$kp = P/4\pi[(z_2-z_1)^2\ (t2-t1)^{-2}] \quad (3)$$

where ka is the rock thermal diffusivity calculated from amplitude (m^2 day^{-1}), kp is the rock thermal diffusivity calculated from the phase lag (m^2 day^{-1}), P is the time period of the thermal wave considered (days), z_1 and z_2 are the measuring depths (m), A_1 and A_2 are the amplitudes of the temperature variations at z_1 and z_2 (°C) and t_2-t_1 is the phase lag during the period P (days).

The thermal offset was calculated as the difference between the mean annual temperature measured at the depth closest to the permafrost table and the mean annual ground surface temperature (MAGST) of sensor A (as the closest to the borehole) (Goodrich, 1982). Potential freeze-thaw events (PFTE) were calculated as the number of times that daily or hourly mean temperature crossed the threshold of 0°C divided per two (Strini et al., 2008).

In order to better describe the environmental conditions, ground thermal regime and the relationships between air temperature and ground surface temperature, the following factors were quantified: i) the degree days of freezing (DDF, sum of degree days below 0°C), ii) the degree days of thawing (DDT, sum of degree days above 0°C), iii) the n-factor (n_t) as the ratio of the degree-day sum at the soil surface to that in the air for the thawing period (following Klene et al., 2001) and, iv) the zero curtain effect period (zc, number of days with persistence of a nearly constant temperature very close to the freezing point, following Outcalt et al., 1990).

A thermal stress index (TSI) was also calculated as the sum of the daily amplitude of the temperature variation (daily maximum - daily minimum) in order to estimate the annual thermal stress due to the daily temperature fluctuations in the rock.

Active-layer thickness (defined as the maximum depth of the 0°C isotherm) was calculated in two different ways:

a) from the intercept of linear regression of the maximum temperature recorded at the borehole between 0.3 and 5 m of depth (Guglielmin et al., 2012a; Adlam et al., 2010) ;
b) the maximum depth of the 0°C isotherm obtained through the interpolation of all the daily maximum temperatures measured in the borehole between 0.02 (thermistor A) and 5 m depth.

Zero Annual Amplitude (ZAA = depth where the difference between the minimum and maximum temperature is smaller than 0.1°C) was calculated following Carlsaw and Jaeger (1959):

$$ZAA = k*P*\pi\ ½ \quad (4)$$

where k is the thermal diffusivity obtained by laboratory analyses, and directly from the temperatures measured in the borehole, and P is the period of the wave (1 year).

Permafrost thickness was calculated following Carlsaw and Jaeger (1959):

$$Zp = MAGT * K*Qg^{-1} \quad (5)$$

where MAGT is the mean annual ground temperature (measured at ZAA), K is the thermal conductivity (W m^{-1} K^{-1}) and Qg is the geothermal heat flux (W m^{-1}). The closest available Qg values range between 63 and 88 mWm^{-2}. The former was derived from ocean drilling boreholes between 64 and 67°S and the latter from a borehole drilled at Bruce Plateau (66°02' S, 64°04' W) on the Antarctic continent (Pollack et al., 1993; Zagorodnov et al. 2012).

Results

Air and Ground surface temperature (GST)

Air temperature data since 1978 are available from the Rothera weather station (AWS) (http://www.antarctica.ac.uk/met/programs-hosted.html), and closely correlate with the air temperature recorded at the permafrost station (PS), that is situated less than 1 km distant and at the same altitude (R^2 = 0.996).

Assuming that the AWS data are representative of the permafrost site, Figure 3 illustrates the strong warming in MAAT over the last 35 years (0.5°C per decade), particularly during the winter (0.8°C per decade), and with summer air warming being much lower (<0.1°C per decade). The spring of 2010 was one of the two warmest in the previous 35 years, .

Air temperature was generally lower than the GST recorded at all three sensors during the summer, while it was roughly equal to the GST at sensor C and higher than GST at sensor A during the winter (Fig. 4a). Air temperature and GST at the three locations showed the lowest correlation at sensor A (Table 1).

The differences among the three sensors are further illustrated in Table 2. Sensor A showed a mean GST during the summer (DJF) ranging between 2.5 and 4.4°C, which is lower up to 3°C than at the other sensor locations. DDT and PFTE were also much lower at sensor A. In addition, Fig. 4b

shows at the ground temperature had more attenuated fluctuations throughout the year at sensor A, where a zero curtain period was also recorded (December 2010).
The n-factor during the thawing season (N_t) at sensor A was roughly 50% lower than at the other sensor locations.
The TSI recorded at sensor A was roughly half (187) that of the other subhorizontal sensor B (300) and only approximately 30% of that of the subvertical sensor C (441), indicating that the thermal stress was much lower at sensor A (table 2).
These characteristics are consistent with the location of sensor A, showing a deeper and more prolonged period of snow cover relative to the other sensors.

Snow variability

Snow depth variability was large both spatially (intra-annual) and temporarily (inter-annual), and dependent on micro topographical characteristics (Figs. 5a,b, Table 3). Among the five points monitored weekly, S2 and S4 showed the greater accumulation. In particular S2 reached a maximum snow thickness exceeding 1 m and experienced a longer duration of snow cover (except during 2010). Snow accumulation was much lower at the remaining three locations with S5 almost always snow-free and S1 and S3 extremely variable interannually both in terms of snow depth and duration. The maximum snow depth ranged between 1 and 142 cm (during 2010), with mean depth ranging between 10 and 21 cm. The number of snow-free days varied widely between years. The points with the largest accumulation did not necessarily show the minimum number of snow-free days (e.g. in 2009, S2 showed greater snow depth than S4 but for a shorter period). The large differences were primarily related to wind redistribution and dependent on the roughness of the surface at meso- (slope scale) and microscale (block scale). Figure 6, illustrates that, after a snow fall event, (indicated by the black arrows) there was normally a period of wind erosion that, in some places, completely removed the new snow as, for example, at the beginning of June 2011, when at S1 the snow depth increased from 0.07 to 0.35 m and then decreased again to 0.07 m in only two weeks (25 May-8 June). This variation is due to the redistribution of the snow, by winds from the northern quadrants (www.antarctica.ac.uk/met/reader). At microscale, as illustrated in Fig. 5a, turbulence can create small snowdrift tails related to the blocks (blue arrows). The melting rate was very similar at all stakes (around 2cm/day during 2010/11 at S1, S2, S4). (Fig. 6). The insulating effect of snow over 0.6 m thick is very clear under both positive or negative air temperatures (Fig. 7). With these values of such snow depth, the positive and negative air temperature peaks were delayed between 2 and 3 days at the surface (e.g. the positive peaks of 16/10 and 4/11/2010 or the negative peaks of 30/10 and 8/11/2010) and the temperature fluctuations at surface were one order of magnitude lower than those in the air. Figure 7 also illustrates that the insulation effect was much reduced with snow thickness under 0.6 m, and the delay was only 1 day (e.g. 13-14/10/2010).

Active Layer and Permafrost

The thermal offset was always negative and generally very small (less than 0.4°C) except in 2009 when it reached -1°C. Ground temperatures within the active layer, showed a progressive delay and smoothing of the fluctuations with increasing depth. The active layer thickness ranged between 76 cm in the summer of 2011/2012 and 140 cm in 2009/2010, showing high temporal variability. Zero curtain periods, indicating ice melting in the rock, were recorded throughout the study between 80 and 130 cm depth, except during the warmest summer (2009-2010) (Fig. 8).
Active layer thickness ranged between 0.76 m in 2012 and 1.4 m in 2010 (Table 4). The maximum depth of the 0°C isotherm calculated through the interpolation of all the daily maximum ground temperature values was very similar to that obtained from the linear interpolation of the annual maximum temperatures at the monitored depths (see Table 4). The thermal diffusivities calculated within the permafrost (below 1.6 m depth) were relatively stable over time at least in the first 15 m,

and generally increased below this depth. Above this depth thermal diffusivity ranged between $2.42*10^{-6}$ and $4.44*10^{-6}$ while below 15 m values were between $1.09*10^{-6}$ and $3.17*10^{-5}$ (Table 4).
The thermal properties calculated in the laboratory from a sample collected at 25 m depth (see Table 5) showed a slight increase in all measured properties with increasing temperature, and the thermal diffusivity was similar to that measured in the borehole below depths greater than 15 m in 2010.
The ZAA depth was shallower in 2009 (14.5 m) and deeper in 2010 and 2011 (16 m), although the temperature was stable around -3°C (Table 4). Permafrost thickness calculations ranged between 112 and 157 m based on the few regional heat flow data values available (Pollack et al., 1993; Zagoridnov et al., 2012) and the thermal conductivity calculated in laboratory at -3°C (Table 5).
The permafrost profile (Fig. 9) included fluctuations below the ZAA that suggest a recent alternation of cooling and warming periods, which may be related with the patterns observed in air temperature in the last 20 years (Fig. 3).
The analysis of the permafrost profile suggests a permafrost thickness greater than that calculated with the thermal conductivity values obtained in laboratory. Assuming a constant thermal gradient below 30 m depth, similar to the mean gradient between 1.6 and 30 m (approximately 0.2°C/10 m) the permafrost thickness could exceed 200 m.

Discussion and conclusions

Relations between snow, air and ground temperature

The strong linear regressions between GST and air temperature for sensors B and C indicate that GST follows the temporal pattern of the air temperature. In both cases ground temperatures were higher than air temperatures except in winter when the solar radiation was minimum. In the location of the sensor A, where the linear regression was much weaker, GST was slightly lower than air temperature except during the mid-summer months, giving a mean annual ground temperature roughly equal to the MAAT (-3.7 vs -3.8°C). All the temperature indices (DDT, n-factor , zero curtain, TSI etc.) are consistent with sensor A having a deeper and more prolonged period of snow cover relative to the other sites. These suggestions are confirmed by the snow data, with sensor A corresponding to the snow cover recorded at the S4, stake while sites B and C were similar to the results of S5 stake. Despite the low relief of the ground, the strong winds typical of this area result in a very large snow cover variability, with the depressed and leeward sites experiencing seven-fold less snow-free days (A) relative to the surrounding more exposed sites.
The net annual effect of snow cover on sensor A was a cooling of the ground surface and, at the same time, reduction in the magnitude of temperature fluctuations. This effect is due to different processes depending on the season time of the year. In summer and to some extent in spring, the main process are i) the insulating effect of the snow cover, ii) the latent heat fluxes due to snow melt and, iii) the higher albedo at sensor A than at the snow free surfaces (Cook et al., 2008). In autumn and, in particular, in winter, when the short wave radiation is minimum, the insulating effect of the snow cover in the study site was exceeded by the net balance of the long wave radiation. With thin snow cover (< 0.2 m), as in location A, the higher emissivity of the snow (0.96-0.98; Zhang, 2005) with respect to the snow-free surfaces (0.91-0.92) results in surface cooling, especially under dry and clear sky conditions. The winter heat loss from the soils in this case is smaller than that reported by Cook et al. (2008) and by Molders and Walsh (2004).
Snow depth and cover variability also have important effects on ecosystems and weathering processes. In locations such as sensor A, snow cover may reduce the potential for freeze-thaw events and thermal stress, while there is also more water available during the melting period. These conditions favour chemical weathering, as noted in several studies (Ballantyne et al. 1985; Hall 1993). The occurrence of late-lying snow patches can create more favourable conditions for mosses or less xeric lichens (Cannone et al., 2006; Kim et al., 2007; Guglielmin et al., 2012b), influencing

the patterns of colonization of the area. Furthermore, colonization by different types of lichen can alter the processes of biochemical and biomechanical weathering (Guglielmin et al., 2012b).

Active Layer and Permafrost

The active layer thickness (ALT) at Rothera Point showed higher temporal variability than that reported from other sites in Maritime Antarctica. For example, in a circumpolar active layer monitoring (CALM) grid at Signy Island (60°43′S, 45°38′W, located at 80 m asl) with an MAAT of -3.7 (Guglielmin et al, 2012a) the ALT ranged between 124 and 185 cm with a maximum interannual difference (MID) of around 30%, while at Rothera Point the active layer ranged between 76 and 140 cm with a MID of more than 44%.

Comparing Rothera with sites in the Northern Hemisphere at similar latitude (Table 6), it is clear that the absolute values of thickness are site specific. The surface characteristics (e.g. density of the vegetation canopy and type) and the active layer characteristics (e.g. the thickness of organic horizon or the ice content), as well as local climatic variables and, in particular, the snow cover are crucial. The two Arctic sites compared here, although having MAAT at least 4°C lower than the Rothera site and a much warmer summer, possessed a thinner active layer and a lower MID because they have a much more developed vegetation canopy and a much thicker organic horizon than at Rothera, where vegetation is almost absent and comprises only epilithic lichens without organic soil horizon. The thicker active layer is also related to the nature of the active layer at Rothera, where there is diorite-granodiorite bedrock with low ice content and high thermal conductivity, while in the Arctic sites sediments generally show a much higher ice content.

Our data series is too short to allow detailed analysis of the relationship between the measured climatic forcing factors (snow cover,depth and persistence, air temperature), GST and ALT. However, high correlations with ALT were found showing: a) an increase of the ALT with increasing mean air temperature in summer (DJF) and b) an increase of the ALT with decreasing maximum snow depth in autumn. The relationship between summer air temperature is commonly reported as the driving climatic influence on ALT and has been noted in many other parts of the world (e.g. Osterkamp 2008; Streletskiy et al., 2008) while, generally, the snow cover exerts a warming effect of especially in the winter in other permafrost areas of the world (e.g. Smith, 1975; Zhang, 2005). The cooling effect of the thin snow cover here exerted during the winter and the spring seem not to have influenced the ALT.

The calculations outlined above suggest that the permafrost depth at Rothera Point is certainly more than 100 m. Large nearshore areas surrounding Rothera Point are <50 m depth, which combined with the deglaciation history of the area (Bentley et al., 2005; Guglielmin et al., 2012b; Hodgson et al., 2013), allow to hypothesize on the possible presence of submarine permafrost in this coastal location, although this has not previously been hypothesised or reported in Maritime Antarctica.

Acknowledgements

We thank the British Antarctic Survey (BAS) for logistic support in the field. We thank again BAS and PNRA (Progetto Nazionale di Ricerca in Antartide) for funding this joint programme of research. We also thank BAS for downloading temperature data and recording snow depth measurements year-round (M. von Tersch, S.J. Duggan, R. Grant, T. Gray). We thank S. Colwell and the SCAR READER database (www. antarctica.ac.uk/met/Reader) for provision of wind data and, finally, three anonymous reviewers and the Guest Editor G. Vieira for their constructive comments.

References

Adlam, L.S., Balks, M.R., Seybold, C.A., Campbell, D.I., 2010. Temporal and spatial variation in active layer depth in the McMurdo Sound Region, Antarctica. Antarctic Science 22, 45–52.

ASTM. 2007. Standard Test Method for Thermal Diffusivity by the Flash Method. ASTM International, West Conshohocken, PA, 2003. DOI: 10.1520/E1461-07 www.astm.org.

Ballantyne, C.K., Black, N.M., Finlay, D.P., 1985. Enhanced weathering under late-lying snowpatches. Earth Surfaces Processes and Landforms 14, 745-750.

Benedict, J.B., 1993. Influence of snow upon rates of granodiorite weathering, Colorado Front Range, USA. Boreas 22, 87-92

Bentley, M.J., Hodgson, D.A., Smith, J.A., Cox, N.J., 2005. Relative sea level curves for the South Shetland Islands and Marguerite Bay, Antarctic Peninsula. Quaternary Science Reviews 24, 1203–1216.

Cannone, N., Ellis Evans, J.C., Strachan, R., Guglielmin, M., 2006. Interactions between climate, vegetation and active layer in maritime Antarctica. Antarctic Science 18, 323–333.

Carlsaw, H.S., Jaeger, J.C., 1959. Conduction of Heat in Solids. Oxford University Press, New York.

Chapin, F.S., Shaver, G.R., Giblin, A.E., Nadelhoffer, K.J., Laundre, J.A., 1995. Responses of Arctic tundra to experimental and observed changes in climate. Ecology 76, 694–711.

Chapman, W.L., Walsh, J.E., 2007. A Synthesis of Antarctic Temperatures. Journal of Climate 20, 4096–4117.

Cook, A.J., Fox, A.J., Vaughan, D.G., Ferrigno, J.G., 2005. Retreating glacier fronts on the Antarctic Peninsula over the past half-century. Science 308, 541–544.

Cook, B.I., Bonan, G.B., Levis, S. Epstein, H.E., 2008. The thermoinsulation effect of snow cover within a climate model. Climate Dynamics 31, 107–124.

Convey, P., Smith, R.I.L., 1997. The terrestrial arthropod fauna and its habitats in northern Marguerite Bay and Alexander Island, maritime Antarctic. Antarctic Science 9, 12–26.

De Pablo, M.A., Blanco, J.J., Molina, A., Ramos, M., Quesada, A., Vieira, G., 2013. Interannual active layer variability at the Limnopolar Lake CALM site on Byers Peninsula, Livingston Island, Antarctica. Antarctic Science 25, 167–180

Dewar, G.J., 1970. The geology of Adelaide Island. British Antarctic Survey Scientific Reports, 57. 66 pp.

Emslie, S.D., 2001. Radiocarbon dates from abandoned penguin colonies in the Antarctic Peninsula region. Antarctic Science 13, 289–295.

Goodrich, L.E., 1982. The influence of snow cover on the ground thermal regime. Canadian Journal of Geotechnics 19, 421–432.

Guglielmin, M., 2004. Observations on permafrost ground thermal regimes from Antarctica and the Italian Alps, and their relevance to global climate change. Global and Planetary Change 40, 159–167.

Guglielmin, M., 2006. Ground surface temperature (GST), active layer and permafrost monitoring in continental Antarctica. Permafrost and Periglacial Processes 17, 133–143.

Guglielmin, M., Balks, M.R., Adlam, L.S., Baio, F., 2011. Permafrost Thermal Regime from Two 30-m Deep Boreholes in Southern Victoria Land, Antarctica; Permafrost and Periglacial Processes 22, 129-139.

Guglielmin, M., Cannone, N., 2012. A permafrost warming in a cooling Antarctica? Climatic Change 111, 177–195.

Guglielmin, M., Worland, M.R., Cannone, N., 2012a. Spatial and temporal variability of ground surface temperature and active layer thickness at the margin of Maritime Antarctica, Signy Island. Geomorphology 155, 20-33.

Guglielmin, M., Worland, R., Convey, P., Cannone, N., 2012b. Schmidt hammer studies in the maritime Antarctic: Application to dating Holocene deglaciation and estimating the effects of macrolichens on rock weathering. Geomorphology 155, 34-44

Hall, K., 1993. Enhanced bedrock weathering in association with late-lying snowpatches: Evidence from Livingston Island, Antarctica. Earth Surface Processes and Landforms 18, 121-129.

Hodgson, D.A., Roberts, S.J., Smith, J.A., Verleyen, E., Sterken, M., Labarque, M., Sabbe, K., Vyverman, W., Allen, C.S., Leng, M.J., Bryant, C., 2013. Late Quaternary environmental changes in Marguerite Bay, Antarctic Peninsula, inferred from lake sediments and raised beaches. Quaternary Science Reviews 68, 216-236.

Kim, J.H., Ahn, I.Y., Lee, K.S., Chung, H.S., Choi, H.G., 2007. Vegetation of Barton Peninsula in the neighbourhood of King Sejong Station (King George Island, maritime Antarctic). Polar Biology 30, 903-916.

Klene, A.E., Nelson, F.E., Shiklomanov, N.I., 2001. The n-factor in natural landscapes: variability of air and soil-surface temperatures, Kuparuk River Basin, Alaska, USA. Arctic Antarctic and Alpine Research, 33, 140–148.

Johansson, M., Callaghan, T.V., Bosiö, J., Åkerman, H.J., Jackowicz-Korczynski, M., Christensen, T.R. 2013. Rapid responses of permafrost and vegetation to experimentally increased snow cover in sub-arctic Sweden. Environmental Research Letters 8 doi:10.1088/1748-9326/8/3/035025

Ling, F., Zhang, T.J., 2006. Sensitivity of ground thermal regime and surface energy fluxes to tundra snow density in northern Alaska. Cold Regional Science Technology 44, 121–130,.

Matsuoka, N., Murton, J., 2008. Frost weathering: Recent advances and future directions Permafrost and Periglacial Processes 19, 195-210.

Molders, N., Walsh, J.E., 2004. Atmospheric response to soil–frost and snow in Alaska in March. Theoretical and Applied Climatolology 77, 77–105.

Morse, P.D., Burn, C.R., Kokelj, S.V., 2012. Influence of snow on near-surface ground temperatures in upland and alluvial environments of the outer Mackenzie Delta, N.W.T. Canadian Journal of Earth Sciences 49, 895-913

Ochyra, R., Smith, R.I.L, Bednarek-Ochyra, H., 2008. The Illustrated Moss Flora of Antarctica. Cambridge University Press, Cambridge, 685 pp.

Osterkamp, T.E., 2008. Thermal state of permafrost in Alaska during the fourth quarter of the twentieth. In: Kane, D.L., Hinkel, K.M., (Eds), Proceedings of the Ninth International Conference on Permafrost, Fairbanks, Alaska, June 29–July. University of Alaska Press, Fairbanks pp. 1333–1338.

Outcalt, S.I., Nelson, F.E., Hinkel, K.M., 1990. The zero-curtain effect: heat and mass transfer across an isothermal region in freezing soil. Water Resources Research 26, 1509–1516.

Paudel, K.P., Andersen, P., 2013. Response of rangeland vegetation to snow cover dynamics in Nepal Trans Himalaya. Climatic Change 117, 149-162.

Pollack, H. N., Hurter, S. J., Johnson. J. R., 1993. Heat flow from the Earth's interior: Analysis of the global data set. Reviews of Geophysics 31, 267–280.

Ramos, M., Vieira, G., 2003. Active layer and permafrost monitoring in Livingston Island, Antarctic. First results from 2000 and 2001. In Phillips, M., Springman, S.M., Arenson, L.U., (Eds.), Permafrost. Proceedings of the Eight International Conference on Permafrost, 21-25 July 2003, Zurich, Switzerland, Balkema – Swets & Zeitlinger, Lisse, pp. 929-933.

Ramos, M.,Vieira, G., Gruber, S., Blanco, J.J., Hauck, C., Hidalgo, M.A., Tomé, D., Neves, M., Trindade, A., 2007. Permafrost and active layer monitoring in the maritime Antarctic: Preliminary results from CALM sites on Livingston and Deception Islands. U.S. Geological Survey and The National Academies, USGS OF-2007-1047, Short Research Paper 070, doi:10.3133/of2007-1047.srp070.

Romanovsky, V.E., Sazonova, T.S., Balobaev, V.T., Shender, N.I., Sergueev, D.O., 2007. Past and recent changes in air and permafrost temperatures in eastern Siberia. Global Planetary Change 56, 399–413.

Rott, H., Skvarca, P., Nagler, T., 1996. Rapid collapse of Northern Larsen Ice Shelf, Antarctica. Science 271, 788–792.

Smith, M. W., 1975. Microclimate influences on ground temperatures and permafrost distribution, Mackenzie Delta, Northwest Territories, Canadian Journal of Earth Sciences 12, 1421–1438

Streletskiy, D.A., Shiklomanov, N.I., Nelson, F.E., Klene, A.E., 2008. Long-term active and ground surface temperature trends: 13 years of observations at Alaskan CALM sites. In: Kane, D.L., Hinkel, K.M., (Eds), Proceedings of the Ninth International Conference on Permafrost, Fairbanks, Alaska, June 29–July, University of Alaska Press, Fairbanks pp.1727–32.
Strini, A., Guglielmin, M., Hall, K., 2008. Tafoni development in a cryotic environment: An example from Northern Victoria Land, Antarctica. Earth Surface Processes and Landforms 33, 1502-1519.
Sturm, M., Racine, C., Tape, K., 2001. Climate change: increasing shrub abundance in the Arctic. Nature 411, 546–547.
Sturm, M., Schimel, J., Michaelson, G., Welker, J.M., Oberbauer, S.F., Liston, G.E., Fahnestock, J., Romanovsky, V.E., 2005. Winter biological processes could help convert Arctic Tundra to Shrubland. Bioscience 55, 17–26.
Throop, J., Lewkowicz, A.G., Smith, S.L. 2012. Climate and ground temperature relations at sites across the continuous and discontinuous permafrost zones, northern Canada. Canadian Journal of Earth Sciences 49, 865-876.
Turner, J., King, J.C., Lachlan-Cope, T.A., Jones, P.D., 2002. Recent temperature trends in the Antarctic. Nature 418, 291–292.
Turner, J., Colwell, S.R., Marshall, G.J., Lachlan–Cope, T.A., Carleton, A.M., Jones, P.D., Lagun, V., Reid, P.A., Iagovkina, S., 2005. Antarctic climate change during the last 50 years. International Journal of Climatology 25, 279–294.
Turner, J., Overland, J.E., Walsh, J.E., 2007. An Arctic and Antarctic perspective on recent climate change. International Journal of Climatology 27, 277–293.
Turner, J., Bindschadler, R.A., Convey, P., di Prisco, G., Fahrbach, E., Gutt, J., Hodgson, D.A., Mayewski, P.A., Summerhayes, C.P., (Eds.), 2009. Antarctic climate change and the environment. Scientific Committee on Antarctic Research, Cambridge, 526 pp.
Turner, J., Barrand, N., Bracegirdle, T., Convey, P., Hodgson, D., Jarvis, M., Jenkins, A., Marshall, G., Roscoe, H., Shanklin, J., French, J., Goosse, H., Guglielmin, M., Gutt, J., Jacobs, S., Kennicutt, C., Masson-Delmotte, V., Mayewski, P., Navarro, F., Robinson, S., Scambos, T., Sparrow, M., Speer, K., Summerhayes, C., Thompson, D., Klepikov, A., 2013. Antarctic climate change and the environment: an update. Polar Record 1-23. doi:10.1017/S0032247413000296.
Vaughan, D.G., Marshall, G.J., Connolley, W.M., Parkinson, C.L., Mulvaney, R., Hodgson, D.A., King, J.C., Pudsey, C.J., Turner, J., 2003. Recent rapid regional climate warming on the Antarctic Peninsula. Climatic Change 60, 243-274.
Vieira, G., Bockheim, J., Guglielmin, M., Balks, M., Abramov, A.A., Boelhouwers, J., Cannone, N., Ganzert, L., Gilichinsky, D., Goryachkin, S., López-Martínez, J., Meiklejohn, I., Raffi, R., Ramos, M., Schaefer, C., Serrano, E., Simas, F., Sletten, R., Wagner, D., 2010. Thermal state of permafrost and active-layer monitoring in the Antarctic: Advances during the International Polar Year 2007-2008. Permafrost and Periglacial Processes 21, 182-197.
Zagorodnov, V., Nagornov, O., Scambos, T. A., Muto, A., Mosley-Thompson, E., Pettit, E. C., Tyuflin, S., 2012. Borehole temperatures reveal details of 20th century warming at Bruce Plateau, Antarctic Peninsula. The Cryosphere 6, 675–686.
Zhang, T., 2005. Influence of the seasonal snow cover on the ground thermal regime: an overview. Reviews of Geophysics 43. RG4002.
Zhang, T., Stamnes, K., 1998. Impact of climatic factors on the active layer and permafrost at Barrow, Alaska. Permafrost and Periglacial Processes 9, 229–246.

Table and Figure Captions

Table 1 Linear regressions between the daily mean air temperature measured at Rothera AWS and Rothera PS.

Table 2 Annual and seasonal means of GST and air temperature at Rothera Point. degree days of thawing (DDT), degree days of freezing (DDF), n-factor for the thawing period (n_t), PFTE (Potential Freezing-Thawing Events), TSI (thermal stress index); ZC (zero curtain days) are also illustrated over the study period. The mean annual GST and air temperature of 2009 show only 323 days because the recording period started on 11 February 2009 (*).

Table 3 Snow variability at the monitoring stakes of Rothera permafrost station (PS). All values recorded at the five stakes have an accuracy of ± 0.02 m and are reported in m.

Table 4 Active layer and permafrost characteristics measured in the Rothera borehole: ALT = active layer thickness calculated by linear interpolation of the annual maximum ground temperatures and between brackets by interpolation of daily maximum temperatures; Thermal offset, thermal diffusivities and Zero Annual Amplitude (ZAA) are calculated as described in the Methods section.

Table 5 Thermal properties obtained by laboratory measurements at different temperatures (see Methods for details).

Table 6 Comparison between different ALT values of Arctic stations with similar latitude and Antarctic stations with similar MAAT. Data from Guglielmin et al., (2012a) for Signy Island and from CALM (Circumpolar Active Layer Monitoring database available - http://www.gwu.edu/~calm/data/north.html) .

Fig. 1 Location of the study area in Antarctica (A) and aerial view of Rothera Point (B) indicating the borehole site (triangle) (Photo M.R. Worland).

Fig. 2 Rothera Borehole site: A) location of the GST thermistors (A,B,C), permafrost temperature profile (BH), air temperature (AT) and snow grid. B) Detail of B-C thermistor location.

Fig. 3 Mean annual air temperature (MAAT) and seasonal means measured since 1980 at the Rothera AWS (data obtained from http://www.antarctica.ac.uk/met/programs-hosted.html).

Fig. 4 Comparison between: a) monthly mean air temperature and daily mean ground surface temperatures (GST) at three different sensors (A, B and C) at Rothera Point. b) daily mean of air temperature and GST from the three different sensors for the period.

Fig. 5 Examples of areal variations of snow cover over time at the monitoring stakes. a) maximum snow cover (2 June 2011). Arrows indicate the snowdrift tails formed due to micromorphology effects on the snow redistribution; b) late lying snow cover (16 December 2011). Blue arrows indicate the snow drift tails formed.

Fig. 6 Example of snow cover variability at Rothera Point between October 2009 and October 2011. Stake S5 is the more similar to sensors B and C, while stake S4 is at site A. S5 is almost all the time snow-free and never exceeds 5 cm of snow, while S4 reached almost 1 m of thickness. Black arrows indicate the main snow fall events.

Fig. 7 Relationships between snow cover, air temperature and GST at Rothera Point. Note the long zero curtain period at the location of sensor A (where stake 4 was also located) and its relation to snow melt from 7 to 29 December. Earlier episodes of positive air temperatures during the spring did not lead to any melting at the ground interface because the thickness of the snow was greater than 80 cm.

Fig. 8 Daily maximum ground temperatures within the active layer at the Rothera borehole. Only during the summer 2009/2010 did the sensor placed at 1.3 m depth record maximum temperatures exceeding 0°C.

Fig. 9 Thermal regime of the Rothera borehole. The ZAA ranged between 14.5 and 16 m depth.

Table 1

	Linear Regression	**R^2**
Site A	GST(A) = 0.947air-0.0165	0.7587
Site B	GST(B) = 1.1863air+1.8279	0.8496
Site C	GST(C) = 1.1877air+2.19	0.8264

Table 2

	MAGST (°C)	**MAM (°C)**	**JJA (°C)**	**SON (°C)**	**DJF (°C)**	**TDD (°C)**	**FDD (°C)**	**N-Factor (n_t)**	**PFTE (n)**	**TSI (°C)**	**ZC (Days)**
2009											
A	-4.8*	-3.3	-9.0	-6.1	4.4	186	1731	2.5	0	73	0
B	-3.6*	-2.7	-9.5	-3.0	5.5	368	1531	4.93	3	155	0
C	-3.1*	-2.3	-9.3	-2.2	5.9	422	1440	5.66	7	246	0
Air	-4.6*	-2.5	-8.9	-5.3	1.2	75	1568	n.d.	11	314	0
2010											
A	-2.9	-3.7	-7.8	-3.1	2.5	321	1371	2.34	2	94	23
B	-1.7	-3.3	-7.7	-1.3	5.3	569	1195	4.14	8	173	0
C	-1.5	-3.0	-7.5	-1.1	5.5	618	1149	4.50	16	252	0
Air	-2.7	-3.0	-6.8	-2.2	1.0	137	1140	n.d.	16	322	0
2011											
A	-3.7	-3.3	-10.2	-5.2	3.3	363	1721	2.69	3	394	10
B	-2.6	-2.7	-9.5	-3.3	4.0	567	1526	4.20	10	570	0
C	-2.3	-2.2	-9.2	-2.8	4.3	605	1143	4.48	11	825	0
Air	-3.9	-2.5	-8.7	-5.4	0.4	135	1541	n.d.	15	468	0
2009-11											
A	-3.8	-3.4	-9.0	-4.8	3.4	290	1608	2.51	1.7	187	11
B	-2.6	-2.9	-8.9	-2.5	4.9	501	1417	4.42	7	300	0

C	-2.3	-2.5	-8.7	-2.0	5.2	548	1344	4.88	11.3	441	0
Air	-3.7	-2.7	-8.1	-4.3	0.9	116	1417		14	368	0

Table 3

	S1	**S2**	**S3**	**S4**	**S5**	**Average**
2009						
Max Snow Height	0.045	0.92	0.07	0.54	0.07	0.11
Mean Snow Height	0	0.31	0.01	0.24	0.01	0.10
S.D.	0.01	0.29	0.02	0.17	0.02	0.33
Snow Free Days	217	56	146	20	189	126
2010						
Max Snow Height	0.81	1.42	0.20	0.98	0.01	0.25
Mean Snow Height	0.19	0.76	0.04	0.28	0	0.21
S.D.	0.25	0.41	0.06	0.32	0	0.68
Snow Free Days	91	13	119	27	267	103
2011						
Max Snow Height	0.35	1.20	0.03	0.40	0.03	0.16
Mean Snow Height	0.11	0.53	0	0.16	0	0.14
S.D.	0.14	0.39	1	0.15	1	0.40
Snow Free Days	96	48	301	89	301	167

Table 4

	ALT (cm)	**Thermal Offset (°C)**	**K (m^2s^{-1}) < 15 m**	**K (m^2s^{-1}) > 15 m**	**ZAA (m)**	**T ZAA (°C)**
2009	96 (93)	-1.0	$3.04x\ 10^{-6}$	$8.96x\ 10^{-6}$	14.5	-3.0
2010	140 (138)	-0.2	$4.44x\ 10^{-6}$	$1.09x\ 10^{-6}$	16	-3.0
2011	95 (89)	-0.3	$2.42x\ 10^{-6}$	$3.17x\ 10^{-5}$	16	-3.1
2012	76 (80)	n.d	n.d	n.d.	n.d.	n.d.

Table 5

T(°C)	**Thermal Diffusivity**	**Specific Heat ($Jg^{-1}K^{-1}$)**	**Thermal conductivity**

	(m²s⁻¹ *10⁻⁶)		(Wm⁻¹K⁻¹)
-3	1.608	0.757	3.293
-1	1.618	0.764	3.343
0	1.621	0.767	3.361

Table 6

Locality	2009	2010	2011	2012
Talnik (67° 20'N)	144	138	144	161
Igarka (67° 28'N)	71	67	70	69
Signy (60°43'S)	161	143	170	200
Rothera* (67°34'S)	96	140	95	76

Figure 1a

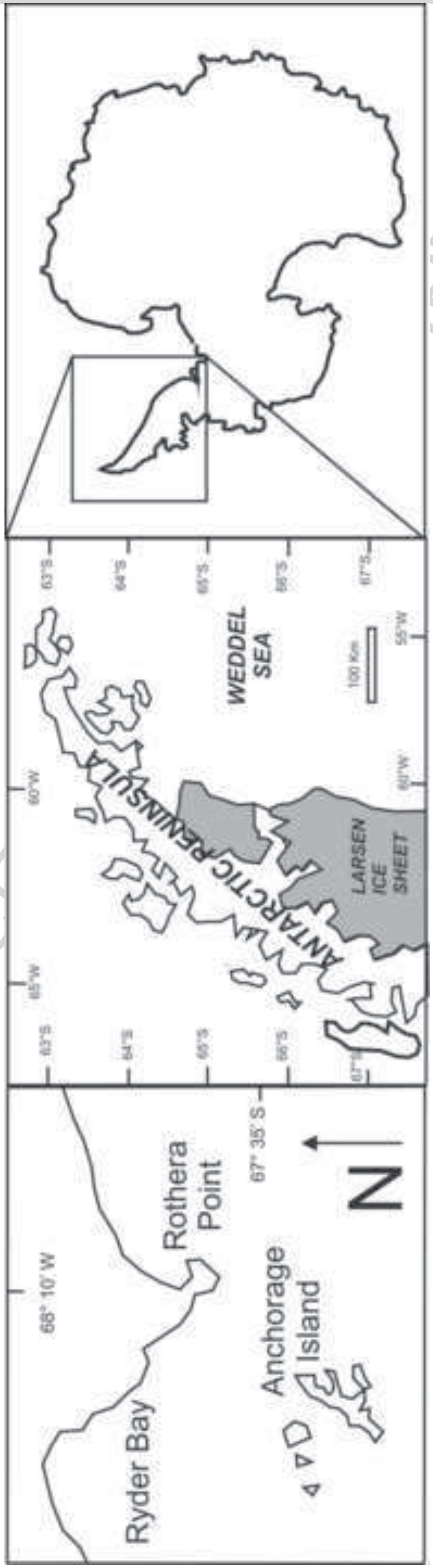
Ryder Bay
68° 10' W
Rothera
Point
67° 35' S
Anchorage
Island
N
63°S
64°S
65°S
66°S
67°S
65°W
60°W
55°W
ANTARCTIC PENINSULA
WEDDEL
SEA
100 Km
LARSEN
ICE
SHEET

Figure 1b

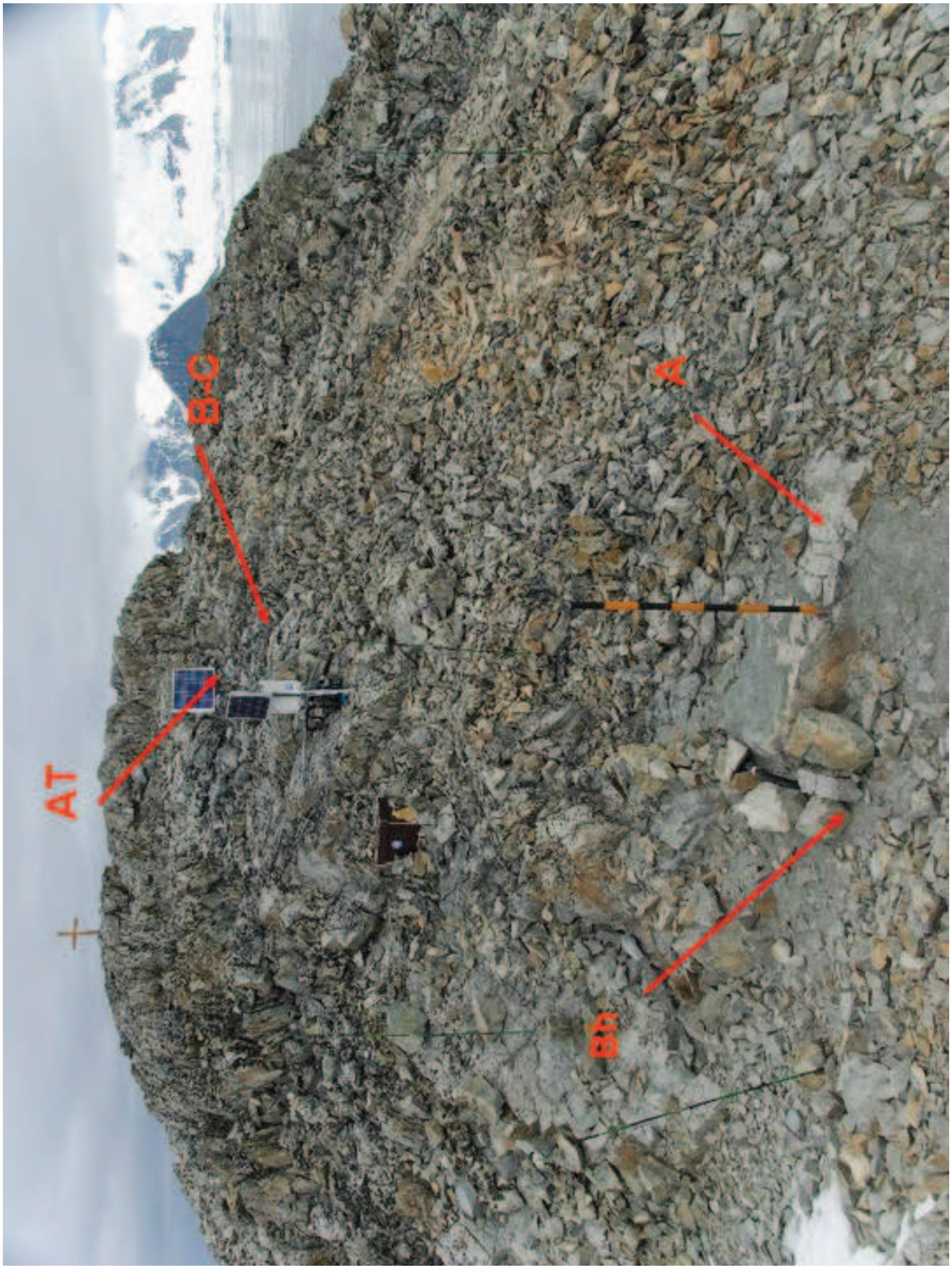

Figure 2a

Figure 2b

Figure 3

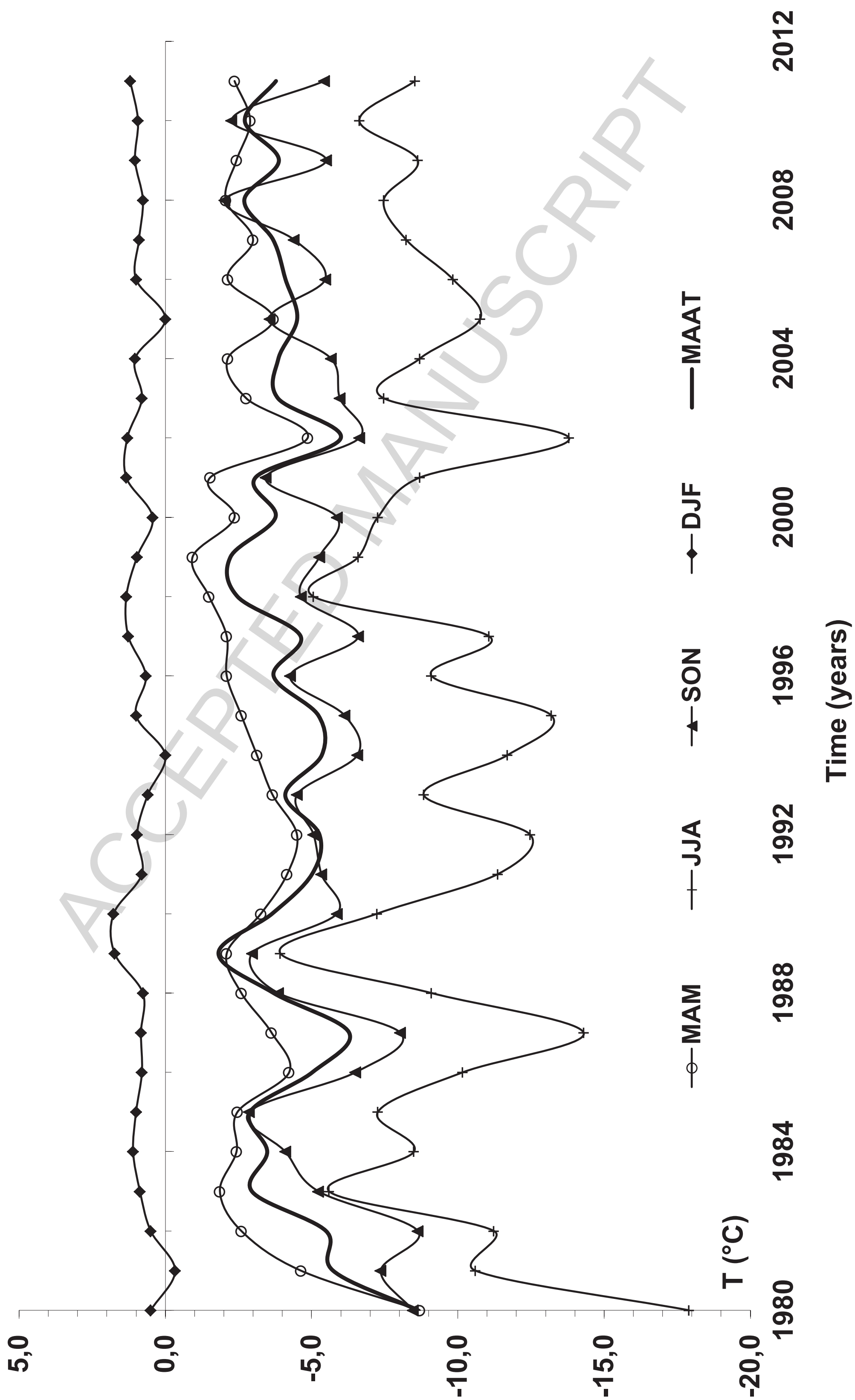
5,0
0,0
-5,0
-10,0
-15,0
-20,0
T (°C)
1980
1984
1988
1992
1996
2000
2004
2008
2012
Time (years)
MAM
JJA
SON
DJF
MAAT

Figure 4a

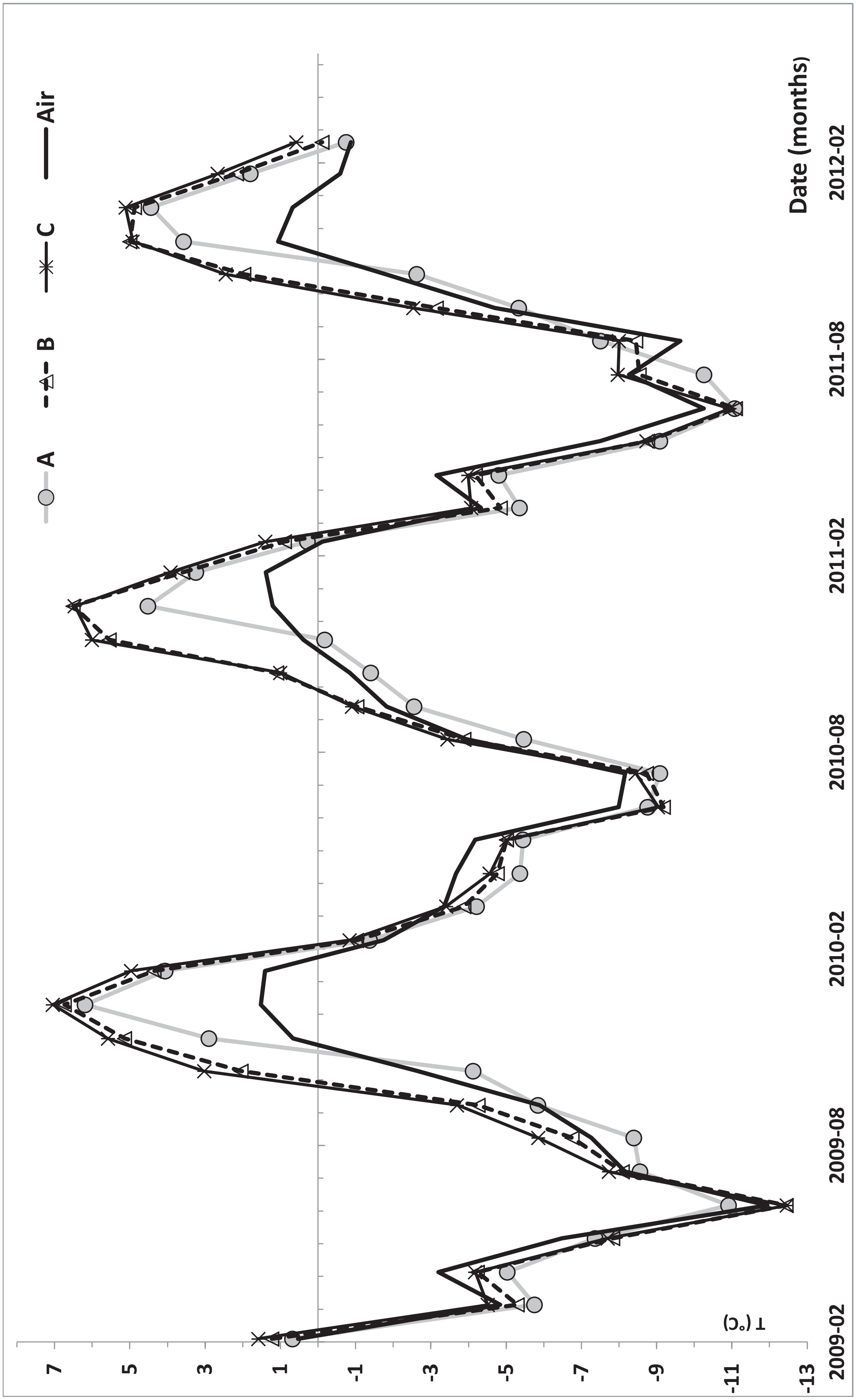
A
B
C
Air
T (°C)
Date (months)
7
5
3
1
-1
-3
-5
-7
-9
-11
-13
2009-02
2009-08
2010-02
2010-08
2011-02
2011-08
2012-02

Figure 4b

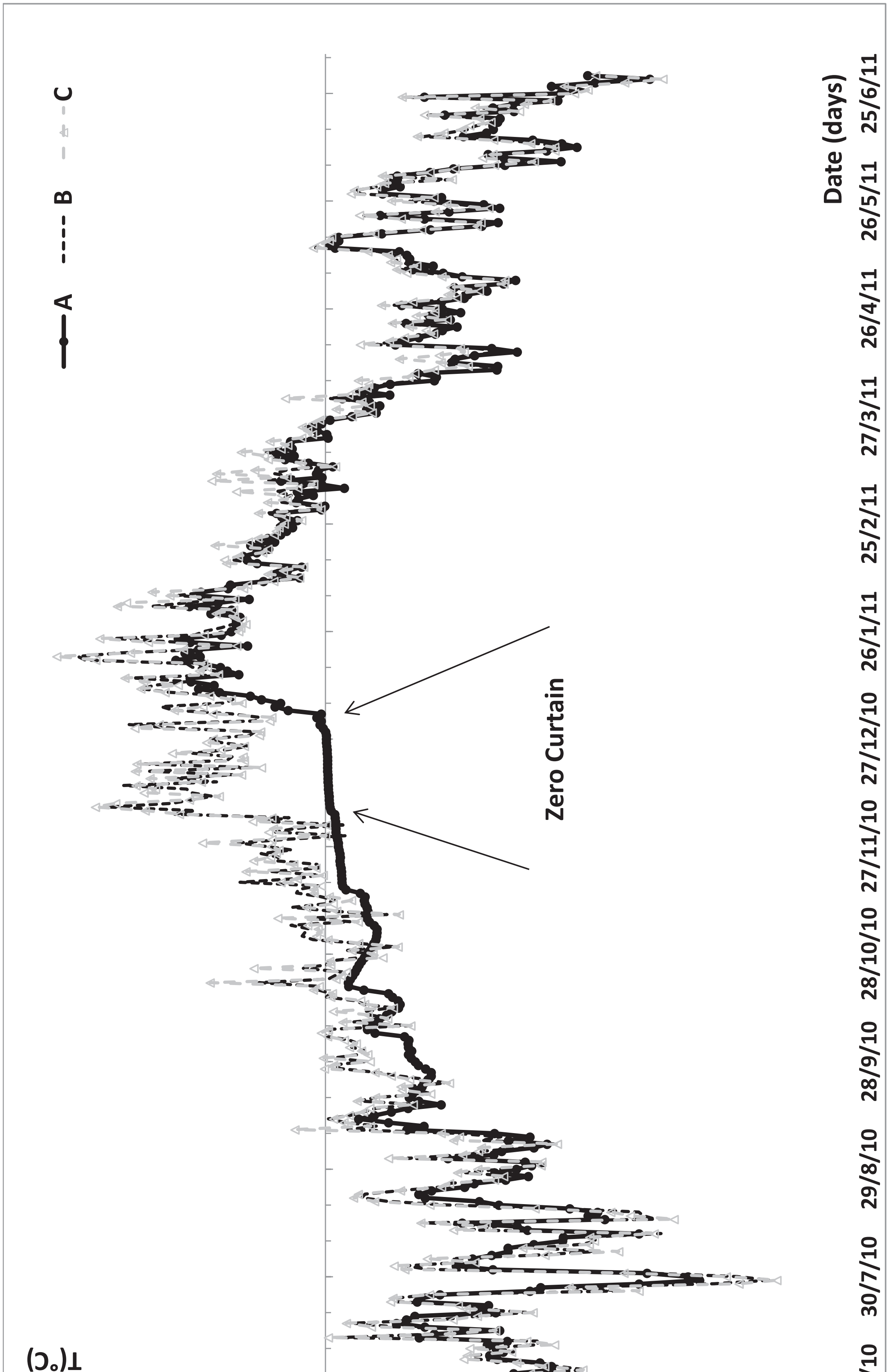
T(°C)
15
10
5
0
-5
-10
-15
-20
-25
A
B
C
Zero Curtain
30/6/10
30/7/10
29/8/10
28/9/10
28/10/10
27/11/10
27/12/10
26/1/11
25/2/11
27/3/11
26/4/11
26/5/11
25/6/11
Date (days)

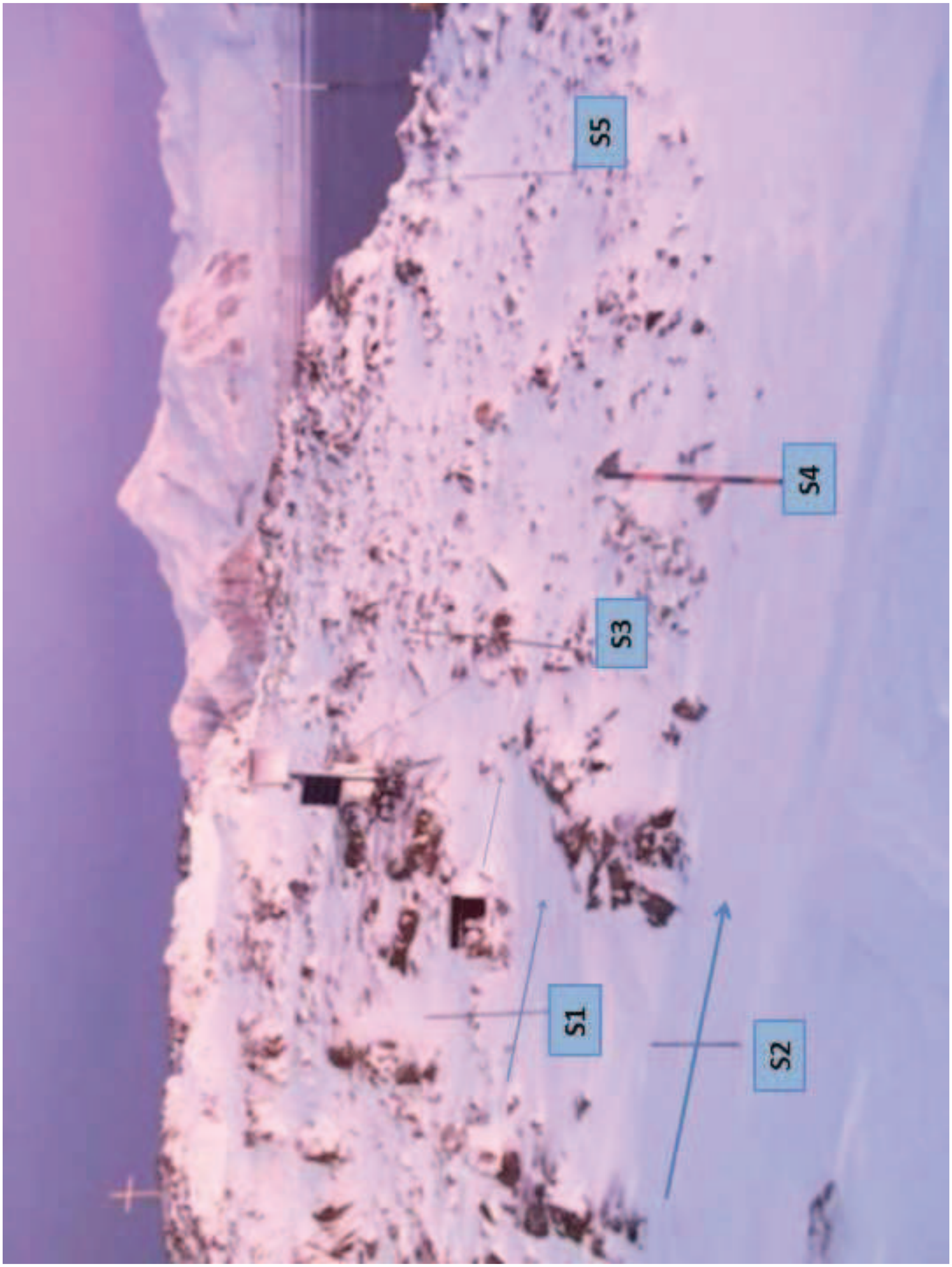

Figure 5a

Figure 5b

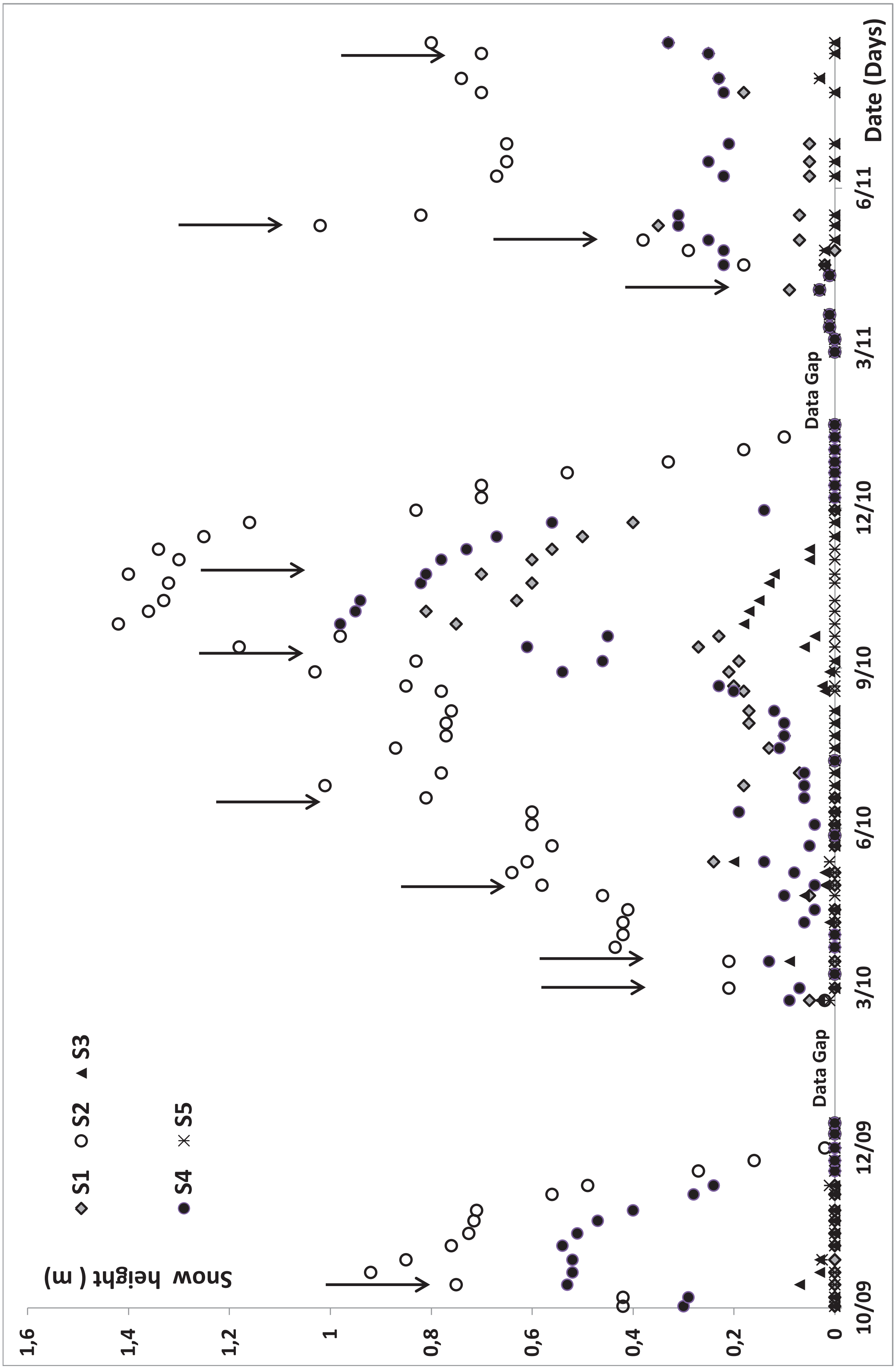
Snow height (m)
1,6
1,4
1,2
1
0,8
0,6
0,4
0,2
0
S1
S2
S3
S4
S5
Data Gap
Data Gap
10/09
12/09
3/10
6/10
9/10
12/10
3/11
6/11
Date (Days)

Figure 6

Figure 7

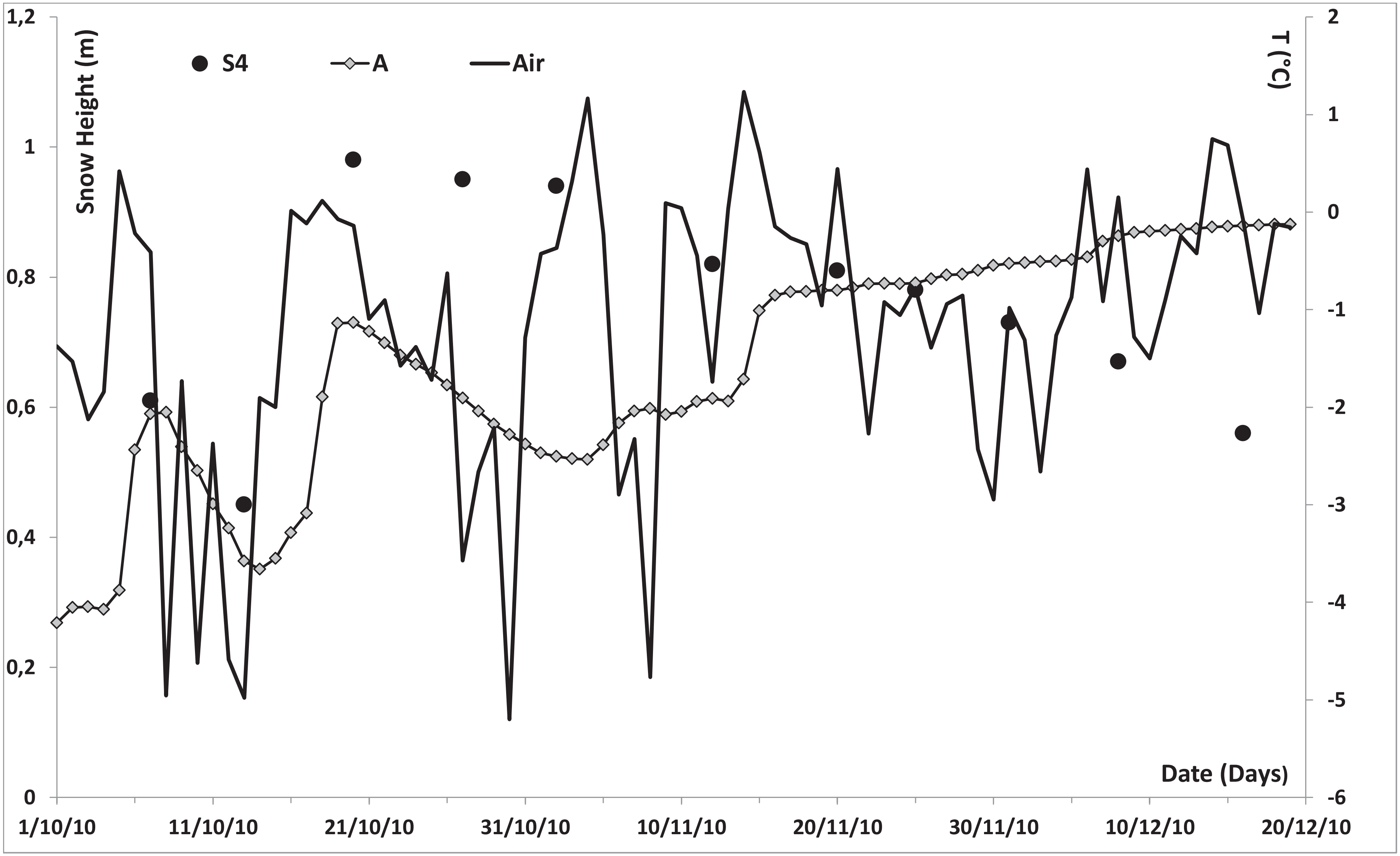

S4
A
Air
Snow Height (m)
T (°C)
Date (Days)
1,2
1
0,8
0,6
0,4
0,2
0
2
1
0
-1
-2
-3
-4
-5
-6
1/10/10
11/10/10
21/10/10
31/10/10
10/11/10
20/11/10
30/11/10
10/12/10
20/12/10

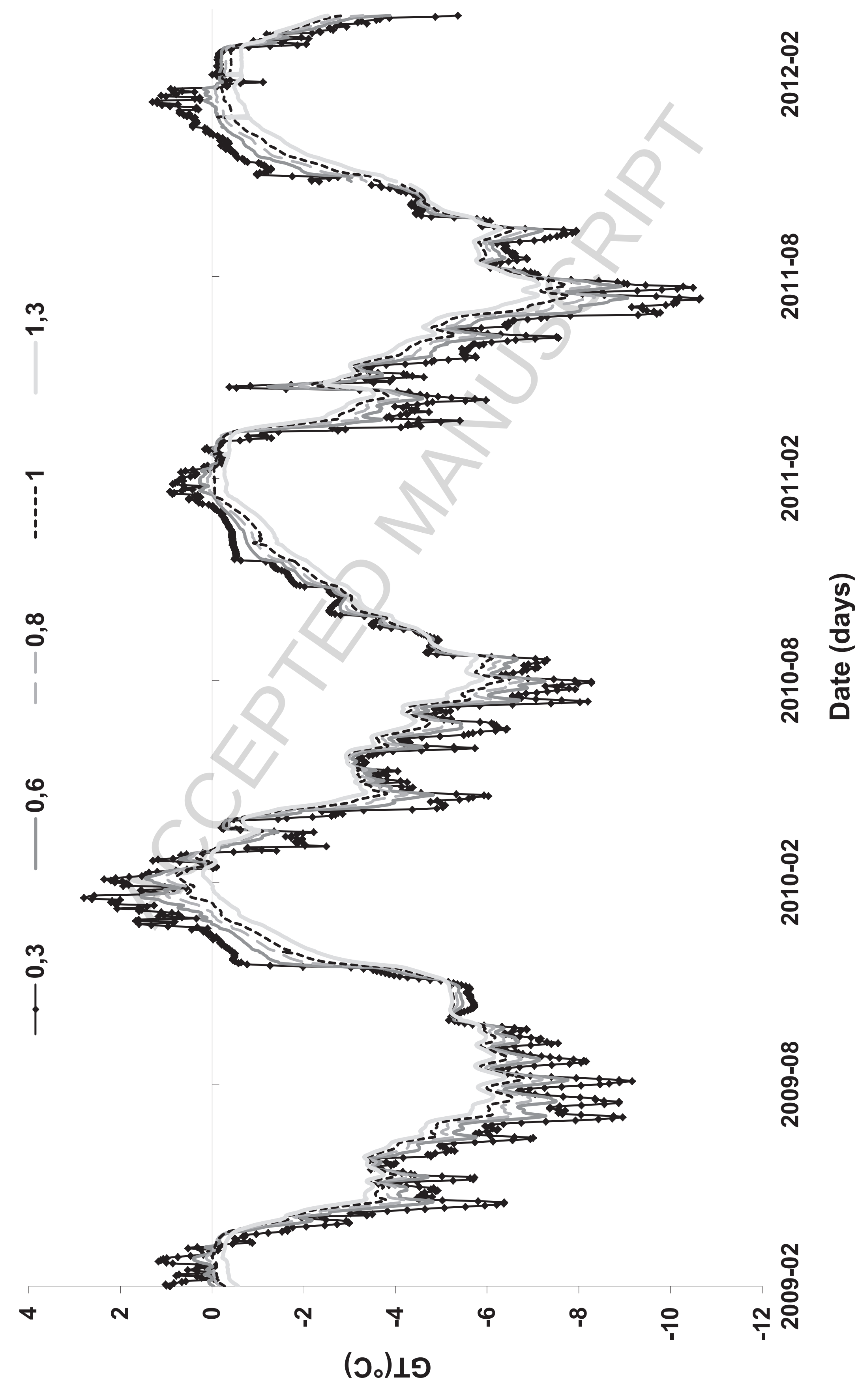

0,3
0,6
0,8
1
1,3
GT(°C)
4
2
0
-2
-4
-6
-8
-10
-12
2009-02
2009-08
2010-02
2010-08
2011-02
2011-08
2012-02
Date (days)

Figure 8

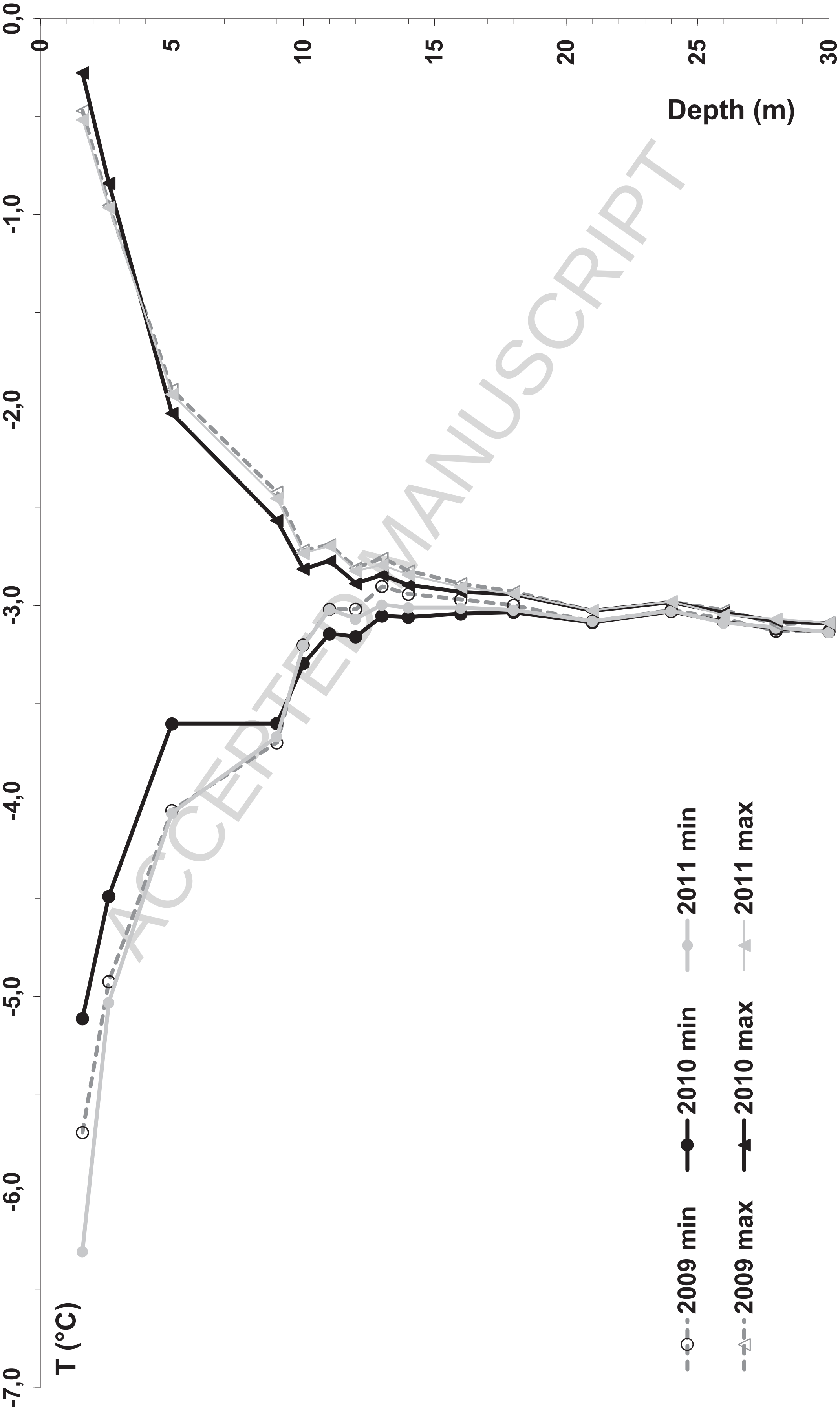

T (°C)
Depth (m)
0,0
-1,0
-2,0
-3,0
-4,0
-5,0
-6,0
-7,0
0
5
10
15
20
25
30
2009 min
2009 max
2010 min
2010 max
2011 min
2011 max

Figure 9